

Pauli Blockade in a Few-Hole PMOS Double Quantum Dot limited by Spin-Orbit Interaction

H. Bohuslavskyi

Université Grenoble Alpes, F-38000 Grenoble, France

CEA, LETI MINATEC campus, F-38000 Grenoble, France and

CEA, INAC-PHELIQS F-38000 Grenoble, France

D. Kotekar-Patil, R. Maurand, A. Corna, X. Jehl, S. De Franceschi, and M. Sanquer

Université Grenoble Alpes, F-38000 Grenoble, France and

CEA, INAC-PHELIQS F-38000 Grenoble, France

S. Barraud, L. Hutin, and M. Vinet

Université Grenoble Alpes, F-38000 Grenoble, France and

CEA, LETI MINATEC campus, F-38000 Grenoble, France

L. Bourdet and Y.-M. Niquet

Université Grenoble Alpes, F-38000 Grenoble, France and

CEA, INAC-MEM F-38000 Grenoble, France

Abstract

We report on hole compact double quantum dots fabricated using conventional CMOS technology. We provide evidence of Pauli spin blockade in the few hole regime which is relevant to spin qubit implementations. A current dip is observed around zero magnetic field, in agreement with the expected behavior for the case of strong spin-orbit. We deduce an intradot spin relaxation rate ≈ 120 kHz for the first holes, an important step towards a robust hole spin-orbit qubit.

Since the proposal of Loss and DiVincenzo in 1998 [1] to make quantum bits based on spins confined in semiconductor quantum dots, substantial progress has been made. First in III-V materials, where the maturity of growth techniques has allowed the emergence of top-down qubits based on the confinement of a two-dimensional electron gas in GaAs/AlGaAs hetero-structures [2], but also of bottom-up qubits made from nanowires (InAs or InSb) [3, 4]. In all III-V qubits, the dephasing time is limited by the interaction of the electron spin with the nuclear spins present in the host material [5, 6]. In contrast silicon, which presents a low natural abundance of nuclear spins and can even be isotopically purified, can be used to make electron spin qubits with extremely long dephasing time [7–10]. An all-electrical control of single dot spin qubit by a single gate voltage microwave signal without the need of local magnetic field gradient [11] would be a clear asset for future developments. Fast and local electrical manipulation using spin-orbit interactions has already been demonstrated in III-V materials. [3, 4]. Thus focusing on holes in silicon appears as an appealing strategy since valence-band holes present a limited hyperfine interaction[12] together with a strong spin-orbit interaction (SOI) due to their p-orbital nature. Recent experiments [13, 14] have indeed revealed SOI-related spin properties and a hole spin qubit has even been demonstrated [15]. Here, we report on the implementation of a silicon hole double quantum dot (DQD) based on the technology described in refs. 16, 17. The device is tunable in the few hole regime in which we investigate Pauli spin blockade (PSB), the key ingredient for spin qubits initialization and readout in several qubit implementations [2]. More specifically, we focus on the magnetic field evolution of the leakage current through the device in the PSB regime. It reveals a dip around zero magnetic field linked to spin-orbit mixing [18]. The spin relaxation rates determined from the PSB are comparable with the values extracted for electrons in InAs nanowire double quantum dots [19] and are compatible with the operation of a hole spin-orbit qubit in silicon [15].

Our devices are nanowire field-effect transistors fabricated in a 300 mm CMOS facility on silicon-on-insulator wafers with 145 nm-thick buried oxide. The 11 nm-thick Si channel is doped with $\simeq 4 \times 10^{24}$ Boron.m⁻³. Nanowire width down to 18 nm are achieved after patterning. Two gates (G1 and G2) in series are patterned by electron-beam lithography and are isolated from the channel by 2.5 nm of SiO₂ and 1.9 nm of HfO₂. Silicon nitride spacers are then deposited and etched on the sidewalls of the gates (see figure 1a,b). The spacers effectively protect the inter-gate spacing from the silicidation and dopant implantation used

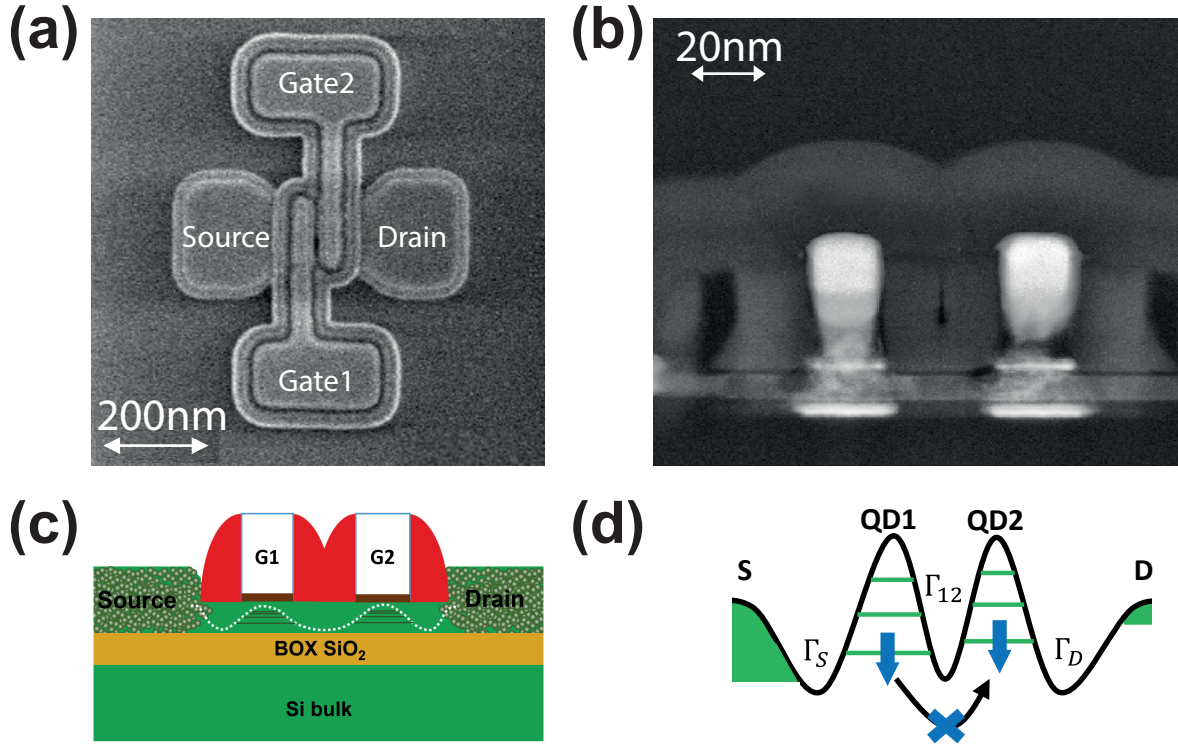


Figure 1: (a) Top view scanning electron micrograph of a typical DQD device after spacer etching, featuring 30 nm-long gates separated by 35 nm. (b) Transmission electron micrograph along the source-drain axis. (c) Schematics of the DQD made by hole accumulation below G1 and G2. (d) Schematic Pauli spin blockade for the $(1h,1h) \rightarrow (0,2h)$ transition at reverse bias ($V_{DS} \leq 0$, analogue to the $(3h,3h) \rightarrow (2h,4h)$ transition in the inset of Fig. 4c). The black line is the top of the valence band. The green regions indicate the hole reservoirs in the source and drain.

to reduce the access resistances [17]. The resulting structure, sketched in figure 1c, yields a compact DQD with optimal gate control. At low temperature, two quantum dots, QD1 and QD2, are formed by accumulation below G1 and G2 respectively (see figure 1c-d). The same process has been used to produce n-type DQD[20].

Electrical characterization was performed from $T=300$ K down to very low temperature by recording the drain-source current I_{DS} as a function of the two gate voltages V_{G1} and V_{G2} (stability diagram) at various drain source voltages V_{DS} . In the experimental setup the source was grounded. The stability diagram shown in fig. 2a reveals overlapped bias triangles [21] with vertical and horizontal edges. This is a characteristic of an excellent electrostatic control of each dot by one gate. The gate capacitances associated to G1 and G2, C_{G1} and C_{G2} are therefore the dominant capacitances and the lever arm parameters $\frac{C_{G1}}{C_{\Sigma 1}}$

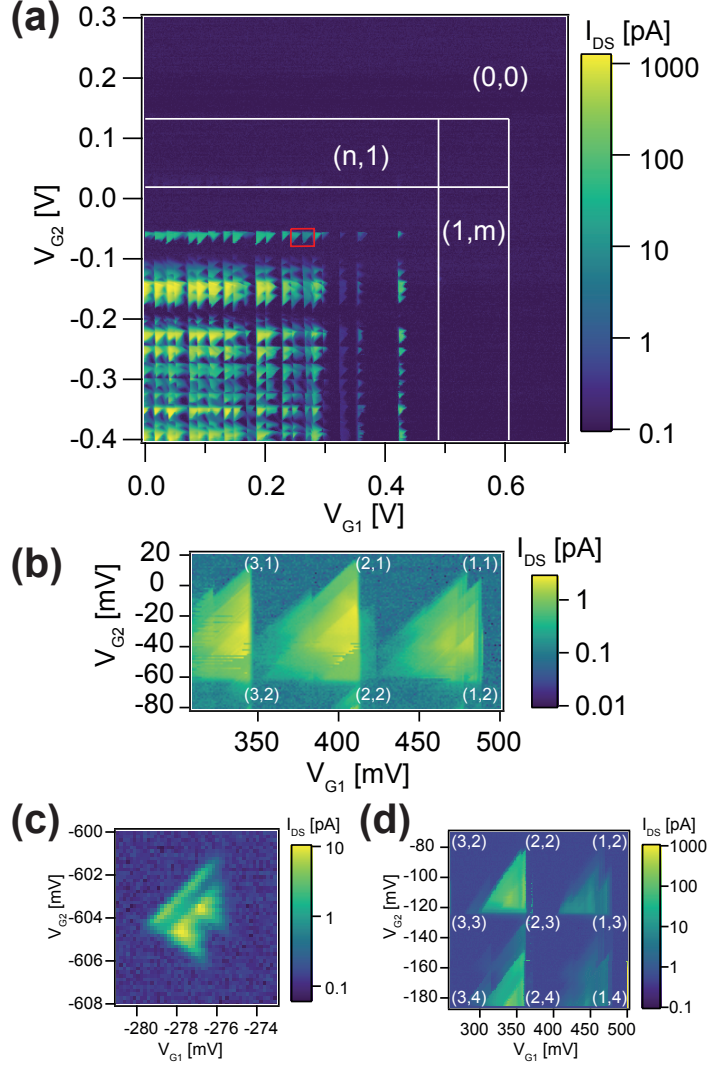


Figure 2: (a) I_{DS} versus V_{G1} and V_{G2} measured with $V_{DS}=20$ mV at $T=60$ mK. White lines indicate the position of four lines of current detected at larger bias (see b). The absolute hole occupation numbers are indicated for the few hole region. The red square indicates the region studied in fig. 3a). (b) I_{DS} versus V_{G1} and V_{G2} measured with $V_{DS}=-100$ mV at $T=60$ mK in a region where no current is detected at $V_{DS}=20$ mV ($(n,1) \rightarrow (n,2)$ transition line). (c) I_{DS} versus V_{G1} and V_{G2} measured with $V_{DS}=-3$ mV at $T=60$ mK in the many hole regime. (d) I_{DS} versus V_{G1} and V_{G2} measured with $V_{DS}=-70$ mV at $T=60$ mK in the region where PSB has been studied (see Fig. 4). The absolute hole occupation numbers are indicated.

and $\frac{C_{G2}}{C_{\Sigma 2}}$ are close to 1 ($C_{\Sigma 1}=C_{G1}+C_S+C_{12}$ and $C_{\Sigma 2}=C_{G2}+C_D+C_{12}$ are the total capacitances for QD1 and QD2, C_{12} being the capacitance between QD1 and QD2 and C_S (C_D) being the source to QD1 (drain to QD2) capacitance).

In order to precisely know (n, m) -the charge state with $n(m)$ excess holes in QD1(QD2)-

a large V_{DS} has been applied. Even if transitions $(1, m) \rightarrow (0, m + 1)$ and $(n, 1) \rightarrow (n + 1, 0)$ have not been detected at $V_{\text{DS}}=20$ mV, they appear above $|V_{\text{DS}}| \approx 100$ mV thanks to the enhanced tunneling through the barriers under the spacers: the latter are markedly tilted at high V_{DS} so that the tunnel transparencies Γ_S, Γ_D increase significantly. In figure 2b, the drain current recorded at $V_{\text{DS}}=-100$ mV is shown in a region where no current is detected at $V_{\text{DS}}=20$ mV. This row of triangles correspond to the second ($1 \rightarrow 2$) transition in dot 2. The conducting parts of the triangles are replicated as a result of the ionization of dopants near the channel at large bias[22].

Interestingly, the charging energies are significantly larger in the few holes (up to 70 meV) than in the many holes regime ($\simeq 20$ meV). We have, therefore, performed tight-binding calculations [23] in a realistic geometry in order to understand the nature of the very first low-lying hole states. The first few holes do not localize in edge states as in Ref. [24] because the channel is doped with Boron atoms and the back gate is grounded, therefore the hole are not pulled in the upper corners. They might rather be bound to clusters of two or more nearby Boron impurities which exist in the doped channel. Assuming a random distribution of Boron atoms, there is indeed $> 50\%$ (resp. $> 95\%$) chance of having at least two impurities closer than $d = 1.5$ nm (resp. $d = 2.5$ nm) under the gate. Configuration interaction calculations show that such clusters show larger binding and charging energies E_c than single impurities ($E_c \sim 75$ meV at $d = 1.5$ nm and $E_c < 60$ meV when $d > 2.5$ nm). The charging energy decreases once the deepest clusters are filled and the confinement gets dominated by the structure and gate fields. Despite doping, the SOI is mostly mediated by the silicon matrix as the probability that the holes sit on the Boron atoms is always small.

Once the first holes are added in the channel the DQD is defined by the geometry of the sample. We have simulated the stability diagram in the $(n, m) \geq (5, 3)$ regime with the orthodox Coulomb blockade theory. We solved the master equation for transport [25] with the parameters given in table I. In addition to the capacitances defined above, we set the electronic temperature T_e , as well as the tunneling rates Γ_S, Γ_D and Γ_{12} associated to C_S, C_D and C_{12} respectively. The simulation, shown in fig. 3b, reproduces the shape of the measured bias triangles.

The value for C_{12} is deduced from the gate voltage separation ΔV_G between the triple points [21] observed at small V_{DS} (see fig. 2c): $\Delta V_G = e \frac{C_{12}}{C_{G1}C_{G2}} \simeq 1.8$ mV. The values of C_{G1} and C_{G2} used in this simulation are in good agreement with a planar model for the

T_e	150 mK
$C_{G1}=C_{G2}$	7.6 aF
$C_S=C_D$	0.15 aF
C_{12}	0.65 aF
$\Gamma_S=\Gamma_D=\Gamma_{12}$	$10^{-4} \frac{e^2}{h}$

Table I: Numerical values used in the simulation of fig. 3b.

gate capacitance of our DQD: $C_{G1(2)} = \frac{\epsilon_0 \epsilon_{SiO_2} A_{1(2)}}{EOT} \approx 11$ aF, where $A_{1(2)}$ is the channel area covered by G1 (G2), and $EOT \simeq 2.9$ is the equivalent oxide thickness nm [26].

We now turn to the investigation of PSB. Spin blockade in a DQD arises when the current involves a transport cycle equivalent to $(0, 1) \rightarrow (1, 1) \rightarrow (0, 2) \rightarrow (0, 1)$ [27]. Since the $(0, 2)$ ground state is a spin singlet, the cycle stops as soon as the DQD enters in a $(1, 1)$ triplet state. The remaining leakage current results from spin relaxation or spin-orbit mixing mechanisms. Depending on the relevant mechanism, the leakage current will behave differently as a function of the magnetic field and detuning [18, 19].

Figs. 4a and 4b present current triangles in which PSB is evidenced at $T = 60$ mK thanks to the magnetic field dependence of the drain-source current. As expected, a reduced current is detected at the base of the bias triangles [2] corresponding to the $(1, 3) \rightarrow (2, 2)$ transition in Fig. 4a and to the $(3, 3) \rightarrow (2, 4)$ transition in Fig. 4b, respectively. Figs. 4c and 4d display the leakage current as a function of the out-of-plane magnetic field, B , and of the detuning axis in the PSB regime of Fig. 4a and Fig. 4b, respectively (detuning axis are indicated by white arrows in Figs. 4a and 4d). The leakage current decreases around $B = 0$ in both cases. The current does not depend on magnetic field for the reverse polarity ($V_{DS} < 0$) as well as for the two other triangles shown in Fig. 2d, i.e. for $(3, 2) \leftrightarrow (2, 3)$ and $(2, 3) \leftrightarrow (1, 4)$ transitions. Note here that the $(1, 1) \rightarrow (0, 2)$ transition - at which PSB is also expected - was not caught even at large bias.

A cut at zero detuning taken in Fig. 4c (in Fig. 4d) is shown in figure Fig. 4e (in Fig. 4f). It reveals a current dip that can be fitted to a Lorentzian function, in line with a model assuming strong SOI [18]:

$$I = I_{\max} \left(1 - \frac{8}{9} \frac{B_C^2}{B_C^2 + B^2} \right) + I_0 \quad (1)$$

with $I_{\max} = 4e\Gamma_{\text{rel}}$ the dip height, where Γ_{rel} is the spin relaxation rate among the $(1, 1)$ states, B_C is the dip width and I_0 is a B-independent background current [13] (0.15 pA for

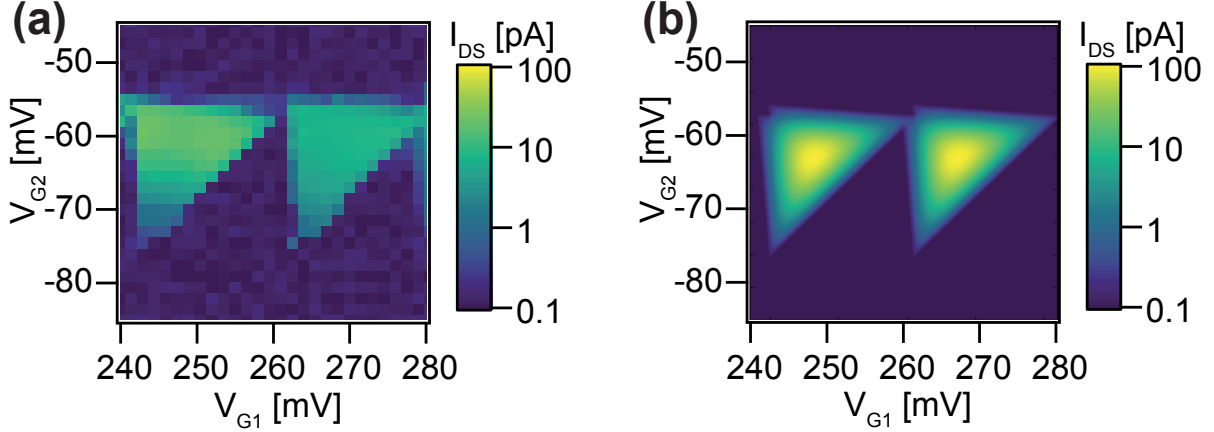


Figure 3: (a) I_{DS} versus V_{G1} and V_{G2} measured with $V_{DS}=20$ mV at $T=60$ mK (region highlighted in red in fig. 2a) (b) Electrostatic simulations with the parameters given in table I.

the $(1,3)\rightarrow(2,2)$ transition and 1.3 pA for the $(3,3)\rightarrow(2,4)$ transition). B_C accounts for the cross-over between leakage currents resulting from spin relaxation at small field and spin-orbit mixing at higher field. The rate Γ_{SO} of spin-orbit mixing between $(1,1)$ states and the $(0,2)$ singlet can be estimated with:

$$g\mu_B B_C \simeq h\sqrt{\Gamma_{rel} \times \Gamma_{SO}} \quad (2)$$

Contrarily to refs. 13, 28, we always see a dip of current at low magnetic field that we attribute to the dominance of spin-orbit mixing over hyperfine [19] or spin-flip cotunneling mechanisms [28, 29]. We also observe two current peaks at $B = \pm 20$ mT and $T = 60$ mK (see Figs. 4c and 4e). Peaks of current at finite magnetic field, whose origin remains unclear, are also reported in refs. 28, 30, 31. The dip observed at zero magnetic field extends in detuning up to several meV, which indicates that the $(0, 2)$ singlet-triplet splitting in our QDs -as other orbital splittings - is large. As a result PSB can be seen even at $T=4.2$ K (not shown).

Γ_{rel} and Γ_{SO} can be estimated from the above experiments. For two QDs in series, Γ_{SO} mainly depends on the interdot coupling. The hole g -factor was found to be anisotropic in similar nanowire transistors [14], with $g = 1.5-2.6$. Eq. (2) then yields $\Gamma_{SO}=1.4-4.3$ meV for the $(1,3)\rightarrow(2,2)$ transition and $\Gamma_{SO}=0.6-1.8$ meV for the $(3,3)\rightarrow(2,4)$ transition. The spin relaxation is dominated by the spin-orbit coupling in our DQD rather than by hyperfine effects. Indeed we estimate a fluctuating Overhauser field $B_{nuc} \approx 20 \mu\text{T}$, which is much

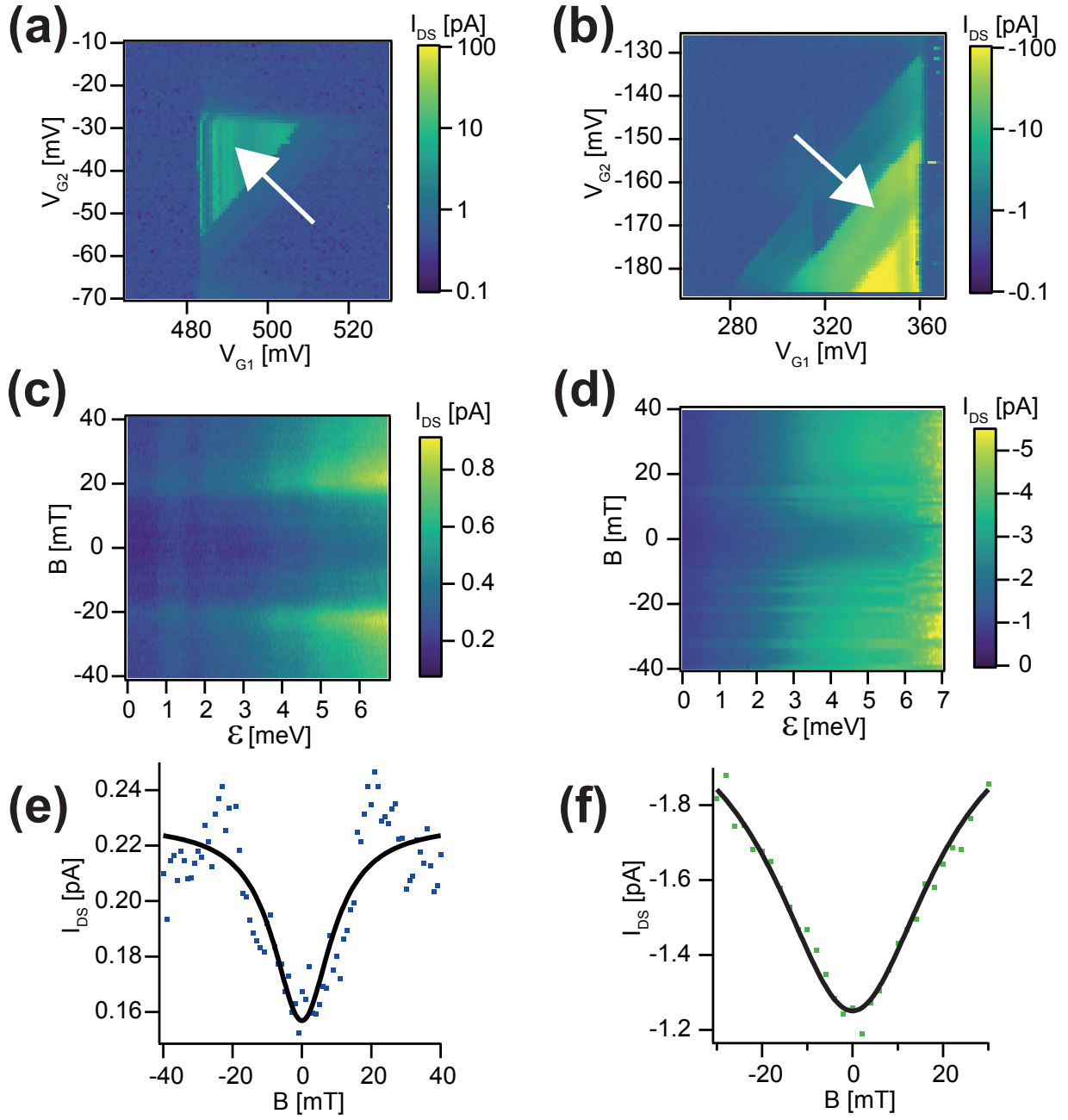


Figure 4: Current in the PSB regime as a function of detuning and out-of-plane magnetic field B at $T=60$ mK. (a) Current versus V_{G1} and V_{G2} at $V_{DS}=70$ mV and $B=0$. (b) Same as in (a) except for $V_{DS}=-70$ mV. (c) Current versus detuning energy ϵ and magnetic field for the $(1,3)\rightarrow(2,2)$ transition (white arrow in a). (d) Same as in (c) but for the $(3,3)\rightarrow(2,4)$ transition (white arrow in b). (e) and (f) are cuts of the $(1,3)\rightarrow(2,2)$ and $(3,3)\rightarrow(2,4)$ transitions at $\epsilon=0$. The curves are fitted (black lines) assuming that PSB is spin-orbit mediated [18].

smaller than the current dip width of 10-20 mT [14, 28]. Γ_{SO} is larger than in previous reports [13, 19] while the critical field B_C is comparable to that of refs. 19, 28 (for electrons) and smaller than in refs. 13, 31 (for holes). This can be attributed to the small value of Γ_{rel} . A large Γ_{SO} can limit qubit readout fidelity through unwanted transitions from (1,1) triplet to (0,2) singlet [32] and it would be favorable to reduce the interdot coupling.

$\Gamma_{rel} = 120$ kHz (resp. 2.0 MHz) for the (1,3) \rightarrow (2,2) (resp. (3,3) \rightarrow (2,4)) transition is smaller than in previous reports [13, 19, 28, 31] where it ranges between 0.8 [28] and 6 MHz [32] (3 MHz in ref. 13, $I_{DS}=6$ pA for $B \geq B_C$ in ref. 31). Γ_{rel} , which limits the inelastic relaxation time T_1 , should be primarily minimized for hole spin-orbit qubits. Contrarily to Γ_{SO} , Γ_{rel} cannot be adjusted by changing the interdot coupling and its optimization is material and process dependent.

To conclude, the few-hole regime has been reached in a silicon CMOS DQD and Pauli spin blockade has been observed at different charge transitions. We found that this blockade is dominated by the SOI. By analyzing the magnetic field evolution of the leakage current in the blockade regime we deduced a small intradot spin relaxation rate (≈ 120 kHz for the first holes), an important step towards a robust hole spin-orbit qubit.

Acknowledgments

The authors thank C. Guedj and G. Audoit for extensive TEM analysis. This work is supported by the EU through the FP7 ICT SiSPIN (323841), SiAM (610637) and H2020 ICT25 MOSQUITO (688539) collaborative projects. Part of the calculations were run on TGCC/Curie thanks to a GENCI allocation.

-
- [1] D. Loss and D. P. DiVincenzo, *Physical Review A* **57**, 120 (1998).
 - [2] R. Hanson, L. P. Kouwenhoven, J. R. Petta, S. Tarucha, and L. M. K. Vandersypen, *Rev. Mod. Phys.* **79**, 1217 (2007), URL <http://link.aps.org/doi/10.1103/RevModPhys.79.1217>.
 - [3] S. Nadj-Perge, S. M. Frolov, E. P. A. M. Bakkers, and L. P. Kouwenhoven, *Nature* **468**, 1084 (2010), ISSN 0028-0836, URL <http://dx.doi.org/10.1038/nature09682>.
 - [4] J. W. G. van den Berg, S. Nadj-Perge, V. S. Pribiag, S. R. Plissard, E. P. A. M. Bakkers, S. M. Frolov, and L. P. Kouwenhoven, *Phys. Rev. Lett.* **110**, 066806 (2013), URL <http://link.aps.org/doi/10.1103/PhysRevLett.110.066806>.

- [//link.aps.org/doi/10.1103/PhysRevLett.110.066806](http://link.aps.org/doi/10.1103/PhysRevLett.110.066806).
- [5] H. Bluhm, S. Foletti, I. Neder, M. Rudner, D. Mahalu, V. Umansky, and A. Yacoby, *Nat Phys* **7**, 109 (2011), ISSN 1745-2473, URL <http://dx.doi.org/10.1038/nphys1856>.
 - [6] G. de Lange, Z. H. Wang, D. Ristè, V. V. Dobrovitski, and R. Hanson, *Science* **330**, 60 (2010), ISSN 0036-8075, URL <http://science.sciencemag.org/content/330/6000/60>.
 - [7] B. M. Maune, M. G. Borselli, B. Huang, T. D. Ladd, P. W. Deelman, K. S. Holabird, A. A. Kiselev, I. Alvarado-Rodriguez, R. S. Ross, A. E. Schmitz, et al., *Nature* **481**, 344 (2012), ISSN 0028-0836, URL <http://dx.doi.org/10.1038/nature10707>.
 - [8] X. Wu, D. R. Ward, J. R. Prance, D. Kim, J. K. Gamble, R. T. Mohr, Z. Shi, D. E. Savage, M. G. Lagally, M. Friesen, et al., *Proceedings of the National Academy of Sciences* **111**, 11938 (2014), URL <http://www.pnas.org/content/111/33/11938.abstract>.
 - [9] E. Kawakami, P. Scarlino, D. R. Ward, F. R. Braakman, D. E. Savage, M. G. Lagally, M. Friesen, S. N. Coppersmith, M. A. Eriksson, and L. M. K. Vandersypen, *Nat Nano* **9**, 666 (2014), ISSN 1748-3387, URL <http://dx.doi.org/10.1038/nnano.2014.153>.
 - [10] M. Veldhorst, J. C. H. Hwang, A. W. Yang, C. H. and Leenstra, B. de Ronde, J. P. Dehollain, J. T. Muhonen, F. E. Hudson, K. M. Itoh, A. Morello, and A. S. Dzurak, *Nat Nano* **9**, 981 (2014), ISSN 1748-3387, URL <http://dx.doi.org/10.1038/nnano.2014.216>.
 - [11] M. Pioro-Ladriere, T. Obata, Y. Tokura, Y.-S. Shin, T. Kubo, K. Yoshida, T. Taniyama, and S. Tarucha, *Nat Phys* **4**, 776 (2008), ISSN 1745-2473, URL <http://dx.doi.org/10.1038/nphys1053>.
 - [12] C. Testelin, F. Bernardot, B. Eble, and M. Chamarro, *Phys. Rev. B* **79**, 195440 (2009), URL <http://link.aps.org/doi/10.1103/PhysRevB.79.195440>.
 - [13] R. Li, F. E. Hudson, A. S. Dzurak, and A. R. Hamilton, *Nano Lett.* **15**, 7314 (2015), ISSN 1530-6984, URL <http://dx.doi.org/10.1021/acs.nanolett.5b02561>.
 - [14] B. Voisin, R. Maurand, S. Barraud, M. Vinet, X. Jehl, M. Sanquer, J. Renard, and S. De Franceschi, *Nano Lett.* **16**, 88 (2016), ISSN 1530-6984, URL <http://dx.doi.org/10.1021/acs.nanolett.5b02920>.
 - [15] R. Maurand, X. Jehl, D. Kotekar Patil, A. Corna, H. Bohuslavskiy, R. Lavieville, L. Hutin, S. Barraud, M. Vinet, M. Sanquer, et al., arXiv:1605.07599 (2016).
 - [16] S. Barraud, R. Coquand, M. Casse, M. Koyama, J. Hartmann, V. Maffini-Alvaro, C. Comboroure, C. Vizioz, F. Aussenac, O. Faynot, et al., *Electron Device Letters, IEEE* **33**, 1526

- (2012), ISSN 0741-3106.
- [17] S. Barraud, R. Lavieville, L. Hutin, H. Bohuslavskiy, M. Vinet, A. Corna, P. Clapera, M. Sanquer, and X. Jehl, *Technologies* **4**, 10 (2016), ISSN 2227-7080, URL <http://www.mdpi.com/2227-7080/4/1/10>.
 - [18] J. Danon and Y. V. Nazarov, *Phys. Rev. B* **80**, 041301 (2009), URL <http://link.aps.org/doi/10.1103/PhysRevB.80.041301>.
 - [19] S. Nadj-Perge, S. M. Frolov, J. W. W. van Tilburg, J. Danon, Y. V. Nazarov, R. Algra, E. P. A. M. Bakkers, and L. P. Kouwenhoven, *Phys. Rev. B* **81**, 201305 (2010), URL <http://link.aps.org/doi/10.1103/PhysRevB.81.201305>.
 - [20] D. Kotekar-Patil, A. Corna, R. Maurand, A. Crippa, A. Orlov, S. Barraud, X. Jehl, S. De Franceschi, and M. Sanquer, arXiv:1606.05855v1 (????).
 - [21] W. G. van der Wiel, S. De Franceschi, J. M. Elzerman, T. Fujisawa, S. Tarucha, and L. P. Kouwenhoven, *Rev. Mod. Phys.* **75**, 1 (2002), URL <http://link.aps.org/doi/10.1103/RevModPhys.75.1>.
 - [22] V. N. Golovach, X. Jehl, M. Houzet, M. Pierre, B. Roche, M. Sanquer, and L. I. Glazman, *Phys. Rev. B* **83**, 075401 (2011), URL <http://link.aps.org/doi/10.1103/PhysRevB.83.075401>.
 - [23] Y. M. Niquet, D. Rideau, C. Tavernier, H. Jaouen, and X. Blase, *Phys. Rev. B* **79**, 245201 (2009), URL <http://link.aps.org/doi/10.1103/PhysRevB.79.245201>.
 - [24] B. Voisin, V.-H. Nguyen, J. Renard, X. Jehl, S. Barraud, F. Triozon, M. Vinet, I. Duchemin, Y.-M. Niquet, S. de Franceschi, et al., *Nano letters* **14**, 2094 (2014).
 - [25] M. Pierre, M. Hofheinz, X. Jehl, M. Sanquer, G. Molas, M. Vinet, and S. Deleonibus, *Eur. Phys. J. B* **70**, 475 (2009), URL <http://dx.doi.org/10.1140/epjb/e2009-00258-4>.
 - [26] M. Hofheinz, X. Jehl, M. Sanquer, G. Molas, M. Vinet, and S. Deleonibus, *Applied Physics Letters* **89**, 143504 (2006).
 - [27] K. Ono, D. G. Austing, Y. Tokura, and S. Tarucha, *Science* **297**, 1313 (2002), URL <http://science.sciencemag.org/content/297/5585/1313.abstract>.
 - [28] G. Yamahata, T. Kodera, H. O. H. Churchill, K. Uchida, C. M. Marcus, and S. Oda, *Phys. Rev. B* **86**, 115322 (2012), URL <http://link.aps.org/doi/10.1103/PhysRevB.86.115322>.
 - [29] N. Lai, W. Lim, C. Yang, F. Zwanenburg, W. Coish, F. Qassemi, A. Morello, and A. Dzurak, *Scientific reports* **1** (2011).

- [30] A. Pfund, I. Shorubalko, K. Ensslin, and R. Leturcq, *Phys. Rev. Lett.* **99**, 036801 (2007), URL <http://link.aps.org/doi/10.1103/PhysRevLett.99.036801>.
- [31] S. V. Pribiag, S. Nadj-Perge, S. M. Frolov, J. W. G. van den Berg, I. van Weperen, S. R. Plissard, E. P. A. M. Bakkers, and L. P. Kouwenhoven, *Nat Nano* **8**, 170 (2013), ISSN 1748-3387, URL <http://dx.doi.org/10.1038/nnano.2013.5>.
- [32] S. Nadj-Perge, V. S. Pribiag, J. W. G. van den Berg, K. Zuo, S. R. Plissard, E. P. A. M. Bakkers, S. M. Frolov, and L. P. Kouwenhoven, *Phys. Rev. Lett.* **108**, 166801 (2012), URL <http://link.aps.org/doi/10.1103/PhysRevLett.108.166801>.